


Kinetic Investigation of Polyurethane Rubber Formation from CO₂-Containing Polyols

Georg A. Buchner¹, Maik Rudolph¹, Jochen Norwig², Volker Marker², Christoph Gürtler², and Reinhard Schomäcker^{1,*}

DOI: 10.1002/cite.201900103

 This is an open access article under the terms of the Creative Commons Attribution License, which permits use, distribution and reproduction in any medium, provided the original work is properly cited.



Supporting Information
available online

A novel CO₂ utilization technology allows for the inclusion of CO₂ as carbonate units and double bond moieties to give additional functionality in polyether polyols. This study examines the chain-elongation kinetics of these diols with diisocyanates to polyurethane rubbers by means of thermal analysis. A reaction order of 1 indicates a strong influence of the chains' mobility on the reaction rate. Spectrometry and comparison with non-double-bond polyols reveal that the effect cannot be attributed to a substantial occurrence of side reactions but is rather due to the intertwining of lengthy chains.

Keywords: CO₂ utilization, Differential scanning calorimetry, Kinetics, Polyurethanes, Rubbers

Received: July 19, 2019; *revised:* November 22, 2019; *accepted:* December 16, 2019

1 Introduction

Carbon capture and utilization technologies have received increasing recognition in the last decade due to their potential contribution to climate change mitigation as well as possible economic benefits [1–3]. One CO₂ utilization technology developed in recent years enables the production of polyether-based polyols with carbon dioxide covalently bound in the polymer backbone as carbonate units [4, 5]. Moreover, it is possible to add functionality to these polyols by copolymerizing double bond (DB) agents such as maleic anhydride [6, 7]. One branch of polyols encompasses bi-OH-functional molecules with low DB contents and molecular weights up to 10 000 g mol⁻¹ [8]. Such polyols can be elongated with diisocyanates to polyurethanes (PUs) in a second process [7, 8]. The resulting material is a synthetic rubber (i.e., (linear) unsaturated polymer chains) that can subsequently be compounded and vulcanized to elastomers [9]; an overview of this three-step process is given in Fig. 1.

An industrially relevant property range for this kind of material was recently confirmed [9]. It displays characteristics of a technical specialty rubber [10]. Proximities in application to nitrile butadiene rubber, ethylene propylene diene monomer rubber, or chloroprene rubber were suggested [9]. In the meantime, polyol and polyurethane have been produced at technical scale [8]. The synthesis of polyol is a sufficiently uniform and well-characterized process; a similar process for CO₂-containing polyols without double bond agents is operated at a scale of 5 kt a⁻¹ in a demonstration plant located in Dormagen, Germany [11–13]. The rubber formation requires a more detailed investigation of

kinetics and thermodynamics to allow for reactor simulation and preparation of scalable process concepts [14]. For this reaction, thermal analysis offers a good choice for simple and quick kinetic investigation [15–17].

In this study, the kinetic behavior of different reaction systems is examined using temperature-programmed differential scanning calorimetry (DSC) measurements. Fourier transform infrared (FTIR) spectroscopy is carried out for examining the conversion and possible side reactions. The polyurethane reaction systems in this paper use polyols as recently introduced. The isocyanate selection follows the economic idea of easy availability and accessibility. The most prominent and by trend most inexpensive diisocyanates are methylene diphenyl diisocyanate (MDI, 65–70 % market share), followed by toluene diisocyanate (TDI, 27–32 % market share), and aliphatic diisocyanates (3–4 % market share) [18]. Most established linear polyurethanes are synthesized with MDI or aliphatic diisocyanates, with hexamethylene diisocyanate (HDI) being the most prevalent aliphatic diisocyanate [18]. Here, the reaction is conducted with HDI and TDI. MDI is omitted in this paper as it is prone to structural alterations which raise the need for additional pretreatment steps and introduce considerable uncertainty.

¹Georg A. Buchner, Maik Rudolph, Prof. Dr. Reinhard Schomäcker schomaecker@tu-berlin.de
Technische Universität Berlin, Department of Chemistry, TC8,
Straße des 17. Juni 124, 10623 Berlin, Germany.

²Dr. Jochen Norwig, Volker Marker, Dr. Christoph Gürtler
Covestro Deutschland AG, Catalysis and Technology Incubation,
Kaiser-Wilhelm-Allee 60, 51373 Leverkusen, Germany.

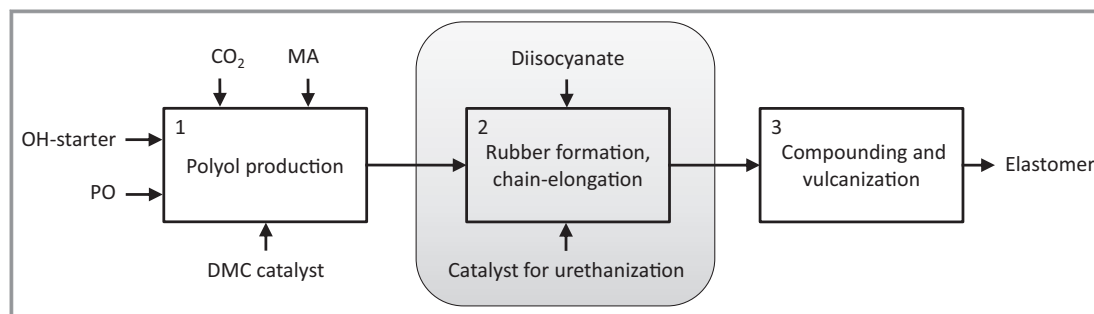


Figure 1. Elastomer production from CO₂-containing polyols, steps: 1) polyol production, 2) polyurethane rubber formation, 3) further processing: mixing, compounding and vulcanization. DMC, double metal cyanide; MA, maleic anhydride; PO, propylene oxide.

2 Experimental Part and Methodology

2.1 Materials and Structures

The examined reaction is a catalyzed polyaddition of diols and diisocyanates to form linear polyurethane chains. Potential side reactions are discussed in Sect. 4. The diols consist of the following building blocks: propylene oxide (PO), CO₂, and maleic anhydride (MA) – the complete molecules of each are included in the polymer chain (structure see Fig. 2, properties see Tab. 1). The polyols were sampled from production in a pilot plant of Covestro Deutschland AG in Leverkusen, Germany. The used isocyanates HDI and TDI were purchased from abcr and Sigma-Aldrich with 98.0 % purity. Dibutyltin dilaurate (DBTL) is employed as catalyst and was purchased from Alfa Aesar and used as received.

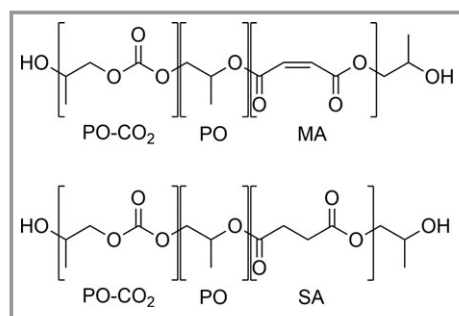


Figure 2. Structures of used polyols, upper: CO₂-MA-PEC1/CO₂-MA-PEC2, lower: CO₂-SA-PEC. PEC, polyether carbonate polyol; MA, maleic anhydride; SA, succinic anhydride; PO, propylene oxide.

2.2 Sample Preparation and Reaction

The polyol was dried in a vacuum dryer at 80 °C and 30 mbar for 24 h before use. DBTL (constant concentration

Table 1. Properties of used polyols. DB, double bond; mPG, monomeric propylene glycol (1,2-propanediol); MA, maleic anhydride; SA, succinic anhydride; PO, propylene oxide.

	Polyol 1	Polyol 2	Polyol 3
Abbreviation	CO ₂ -MA-PEC1	CO ₂ -MA-PEC2	CO ₂ -SA-PEC
Molecular weight M_w [g mol ⁻¹]	4000–4200	3400–3600	2600–2800
Functionality F [-]	2	2	2
DB agent/co-monomer	MA	MA	SA
DB agent/co-monomer content [wt %]	8–9	9–10	5–7
DB content [wt %]	2.1–2.4	2.4–2.7	n.a.
CO ₂ content [wt %]	17–22	14–19	15–20
Starter	mPG	mPG	mPG
Epoxide	PO	PO	PO

for Sects. 3.2 and 3.3 with 50 ppm < c_{DBTL} < 500 ppm and varied for Sect. 3.4) and the polyol were weighed into a 50-mL screw cap container and speedmixed (Hauschild DAC 150, 1 min, 3000 rpm). Immediately after mixing, the container was cooled to approximately -25 °C. Then, the diisocyanate was added, isostochiometrically for Sects. 3.2 and 3.4 and varied for Sect. 3.3, and premixed by hand. Again, the reaction mixture was speedmixed (Hauschild DAC 150, 1 min, 3000 rpm) and instantly cooled down to approximately -25 °C. For the DSC analyses, 10- to 20-mg samples were taken and sealed in aluminum sample pans. The measurements were performed in a Perkin Elmer Pyris 6. The temperature program featured holding 1 min at 30 °C, a heating ramp of 5, 10, 15, and 20 K min⁻¹ to 200 °C and cooling to 30 °C with 50 K min⁻¹. A list of measurements with respective reaction temperature ranges is given in the Supporting Information (Tab. S1). The FTIR spectrometer, a Bruker Vector 22, was equipped with a diamond attenuated total reflection unit. The measurements were performed prior to and after DSC measurements to examine the conversion and possible side reactions via Lambert-Beer law. The solubility of PU rubbers after reaction in the

DSC is examined in dimethylacetamide, dimethyl sulfoxide, *N*-methyl-2-pyrrolidone, and tetramethylurea via IR spectroscopy. The PU rubbers were stirred at 60 °C for 16 h, using 15 mg in 1 g of solvent.

2.3 Kinetic Model and DSC Analysis

For the kinetic analysis, model-free kinetics, e.g., including a variable activation energy, are avoided as they can only describe a system but not mirror meaningful parameters and, thus, not explain a chemical reaction's behavior. Instead, a simple power law model with Arrhenius behavior is taken for a first description (Eqs. (1)–(6)) which allows for the use of the conversion as obtained from thermal analysis.

Power law model kinetics:

$$r_i = -\frac{dc_i}{dt} = k \prod c_i^{n_i} \quad (1)$$

Definition of conversion:

$$X = \frac{c_0 - c}{c_0} \quad (2)$$

Arrhenius:

$$k = Z e^{-\frac{E_A}{RT}} \quad (3)$$

Conversion; Eqs. (2) and (3) in Eq. (1):

$$\frac{dX}{dt} = Z e^{-\frac{E_A}{RT}} (1 - X)^n \quad (4)$$

Conversion; Eq. (4) adjusted for stoichiometry variation:

$$\frac{dX}{dt} = Z e^{-\frac{E_A}{RT}} (1 - X)^{n_1} (1 - \lambda X)^{n_2} \quad (5)$$

Conversion; Eq. (4) adjusted for catalyst concentration:

$$\frac{dX}{dt} = Z' e^{-\frac{E_A}{RT}} (1 - X)^n c_{\text{cat}}^m \quad (6)$$

The values of the conversion rates dX/dt are taken from DSC measurements: the conversion over time and temperature is calculated as respective fractions of the total reaction heat released [19, 20] (the reaction heat is assumed to be independent of the temperature in the examined range). Thermal analysis provides the differential power requirement for heating the sample; after subtraction of the baseline (assumed to be linear as heat capacity and thermal conductivity changes during the reaction can be neglected), the differential power generated by the reaction is obtained; multiplication with time steps yields the differential heat released; normalization to the whole peak's area yields the differential conversion which is finally integrated to obtain the conversion as a function of time.

3 Results

3.1 Ex Situ Analytics

The IR data indicate the necessity of drying the polyol prior to sample preparation as water reacts with the isocyanate groups, forming urea (see Figs. 3 and 5). Drying of about 250 g of polyol removed up to 1 g of water. The high molecular weight of the polyol leads to a relatively small number of functional groups in the reaction mixture for the polyaddition reaction. Thus, small amounts of moisture cannot be neglected. Alcohol and urethane groups could not be quantified via IR due to insufficient signals resulting from very low concentrations (Fig. 3).

For all stoichiometric reaction mixtures, no isocyanate signal could be observed after the reaction, indicating full conversion. Nonstoichiometric reaction mixtures with isocyanate excess show unreacted isocyanate bands, corresponding with the amounts of unreacted isocyanate that is expected if only the main reaction occurs. Analyses in solution, such as gel permeation chromatography, were excluded as the samples could not be dissolved after the reaction. Although by eyesight the samples seemed to be soluble as they were transparent samples after swelling, IR spectroscopy disproved that presumption.

3.2 Polyol and Isocyanate Type Variation

For this section, CO₂-MA-PEC1 and CO₂-SA-PEC are reacted with 1) HDI and 2) TDI, with a constant weight fraction of DBTL as catalyst. Fig. 4 exemplifies the fits of the simulated data to the experimental data. The conversion over time is an S-curve-shaped function which depends on the heating ramp. The faster the heating ramp, the earlier the reaction starts and progresses, in an exponential manner. The results of this variation are listed in Tab. 2.

For the example systems CO₂-MA-PEC1/HDI 1:1 + catalyst and CO₂-MA-PEC1/TDI 1:1 + catalyst shown in Fig. 4, the overall fit quality is convincing with the set of parameters presented in Tab. 2. Due to the high sensitivity of the exponential Arrhenius behavior to the temperature, the simulations by trend start off quicker than the experimental data, whose onset is slightly delayed, but after about 15 % conversion closely follows the model description during the course of the reaction. This behavior is exemplary for all reactions; with the exception of slow heating ramps with TDI whose simulated curve is slightly shifted toward lower conversion. In the experiments with TDI, a two-stage behavior is observed, owing to the different reactivities of the NCO groups in para and ortho positions, with the reaction of the NCO group in ortho position being shifted toward higher temperatures due to steric hindrance. As a consequence, the data are fitted with two reactions as shown distinguished in Tab. 2.

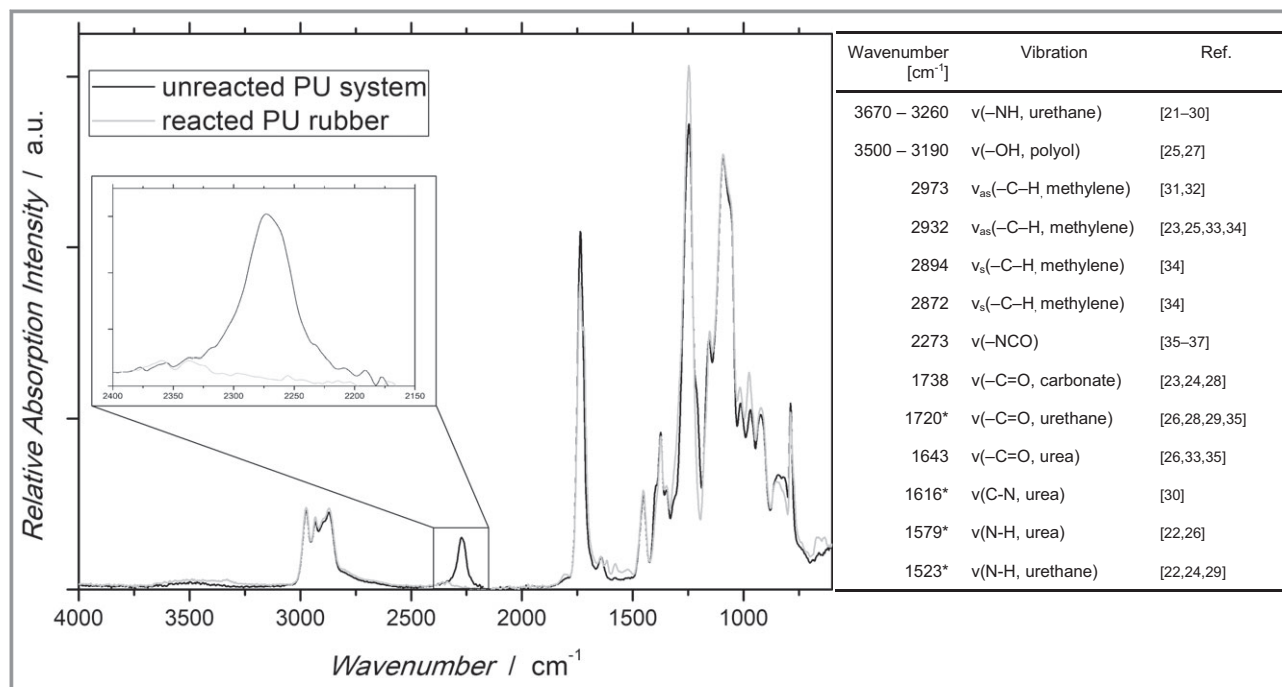


Figure 3. IR spectra of unreacted PU system and reacted PU rubber, isocyanate peak magnified, with vibration assignments, marked (*) wavenumbers are applicable only for the reacted PU rubber system.

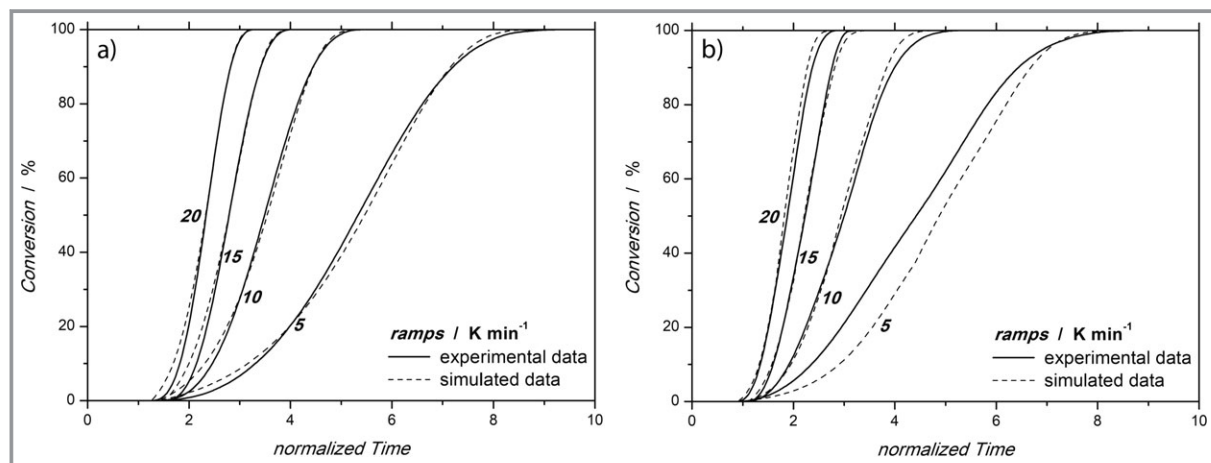


Figure 4. Fit examples, conversion over time, normalized depictions (dimensionless time), heating ramps of 5, 10, 15, and 20 K min⁻¹, DBTL as catalyst. a) System CO₂-MA-PEC1/HDI 1:1 + catalyst, b) system CO₂-MA-PEC1/TDI 1:1 + catalyst.

The kinetic parameters of the systems with double bonds (CO₂-MA-PEC1) and without double bonds (CO₂-SA-PEC) are almost identical. Differences can be explained by baseline and onset selections as well as general measurement accuracy. Both NCO groups of TDI come with higher activation energies, with the ortho reaction's being about 25 % higher. Moreover, it is observed that the reaction with the NCO group in para position is about seven times as fast as the reaction with the NCO group in ortho position and about twice as fast as the reaction with the NCO groups of HDI ($r_{0, \text{norm}, 100^\circ\text{C}}$). It is assumed that the reactions of both

NCO groups of TDI have the same reaction enthalpy (see also [15]).

3.3 Influence of Stoichiometry Variation

The model applied in the previous section includes an overall reaction order but does not distinguish between concentration influences of OH and NCO groups. To gain insights in the contributions of the functional groups to the overall reaction order, the kinetic behavior with varying

Table 2. Summary of kinetic parameters for comparison of polyols with double bonds (CO₂-MA-PEC1) and without double bonds (CO₂-SA-PEC), experiments with HDI and TDI, DBTL as catalyst, DSC analysis, kinetic model following Eq. (4), Z values normalized to system CO₂-MA-PEC1/HDI 1:1 + catalyst, ranges of validity see Tab. S2.

Exp. no.	Polyol	Diisocyanate	NCO pos.	$\Delta_R H$ [kJ mol ⁻¹]	$\log(Z_{\text{norm}}) + 1$ [-]	E_A [kJ mol ⁻¹]	n [-]
A	CO ₂ -MA-PEC1	HDI	-	-18.703	1.00	51.293	0.831
B	CO ₂ -SA-PEC	HDI	-	-30.025	0.99	51.134	0.851
C	CO ₂ -MA-PEC1	TDI	para	-34.194	3.50	67.182	0.922
C	CO ₂ -MA-PEC1	TDI	ortho	-34.194	5.47	87.565	1.129
D	CO ₂ -SA-PEC	TDI	para	-29.213	3.76	68.753	0.804
D	CO ₂ -SA-PEC	TDI	ortho	-29.213	4.85	82.472	1.155

stoichiometry was examined in a second set of experiments (concentration range: 0.047 to 0.922 mmol(NCO) g(system mass)⁻¹). It was found that an additional conversion term in the reaction rate with a separate reaction order (see Eq. (5)) does not improve the fit quality. Rather, it was found that the simple model fits remain satisfying even if the stoichiometric ratio is varied; the results show a similar overall reaction order in all cases. Thus, it is not necessary to modify the conversion term with a coefficient quantifying the stoichiometric imbalance. The fit was then repeated, keeping the simple model with a single reaction order, to check if considerable deviations in the rate constant occur. Deviations in the pre-exponential factors and activation energies in this analysis are attributed to fitting slightly different curvatures due to baseline and onset selections; they approximately cancel each other out for the reaction rate in the relevant temperature range: the resulting initial reaction rates (at 100 °C) are similar for all stoichiometry variations. Tab.3 lists the respective stoichiometry variations carried out and resulting model parameters.

Table 3. Summary of kinetic parameters from stoichiometry variation experiments, HDI + CO₂-MA-PEC1 + catalyst, DBTL as catalyst, DSC analysis, kinetic model following Eq. (4), Z values normalized to system CO₂-MA-PEC1/HDI 1:1 + catalyst, ranges of validity see Tab. S2.

Exp. no.	OH/NCO	$\Delta_R H$ [kJ mol ⁻¹]	$\log(Z_{\text{norm}}) + 1$ [-]	E_A [kJ mol ⁻¹]	n [-]
E	10:1	-12.863	0.91	48.980	0.831
F	5:1	-9.079	2.77	62.253	0.831
G	2:1	-7.456	1.35	52.764	0.831
H	1:1.5	-22.509	1.90	56.783	0.831
I	1:2	-23.778	1.40	53.341	0.831

3.4 Influence of Catalyst Concentration

The influence of the catalyst concentration is examined in an industrially relevant range. Three catalyst concentrations with four heating ramps each were simultaneously fitted. An order of 0.582 for the catalyst concentration was found. The resulting kinetic parameters for the respective experiments are listed in Tab. 4.

Table 4. Summary of kinetic parameters from stoichiometry variation experiments, HDI + CO₂-MA-PEC2 + catalyst, DBTL as catalyst, DSC analysis, kinetic model following Eq. (6), $Z = Z' c_{\text{cat}}^m$, Z values normalized to system CO₂-MA-PEC1/HDI 1:1 + catalyst, ranges of validity see Tab. S2.

Exp. no.	$c_{\text{cat, norm}}$ [-]	$\Delta_R H$ [kJ mol ⁻¹]	$\log(Z_{\text{norm}}) + 1$ [-]	E_A [kJ mol ⁻¹]	n [-]	m [-]
J	0.5	-28.560	1.16	52.970	0.87	0.582
K	1.0	-22.752	1.33	52.970	0.87	0.582
L	2.0	-24.168	1.51	52.970	0.87	0.582

4 Discussion

4.1 General Considerations

Two different types of deviations from the working hypothesis occur in this study and are discussed in this part: first, a lack of sufficient explanation of measured data with the chosen model description, i.e., deviations between the fitted curves and experimental results; second, differences in found parameter values to initial expectations. A multitude of reasons can be distinguished and can be sorted into the following groups: general approach and model form, chemical reasons, i.e., the reaction network that is directly affecting the stoichiometry, or physical reasons, i.e., mass transport. As for the general approach, both power law models and Arrhenius behavior have proven to accurately describe the microkinetics of thermochemical reactions; they are frequently used with satisfying agreement and, thus, can be excluded from the following discussion.

4.2 Chemical Effects: Reaction Network

With respect to the reaction network, a variety of reactions (1 to 7) can affect the availability of the OH and NCO functional groups. 1) First, the polyol has both primary and secondary OH functionalities, which can have different kinetic

behavior due to steric hindrance. While the reactivity of OH groups with isocyanates is reported to generally decrease in the order primary > secondary > tertiary [38], differences are not observed in fast reactions, e.g., demonstrated for shorter diols in [37, 38]. For the examined polyols, no detailed composition data are given. In the experimental data, differences between primary and secondary OH groups could not be observed; the inclusion of two different reactions has no effect on the fit. 2) In experiments with TDI, the NCO group in para position reacts about 7 times as fast as the NCO group in ortho position (8.3 is reported in [18]); this is due to their different steric situations with about 20 % lower activation energy. It is generally agreed in literature that aromatic isocyanates show faster reactions due to lower activation energy [38–40]. In this study, it is found that under the same conditions and in a relevant temperature range, the reaction of the NCO group in para position is faster than the HDI's NCO groups, while the reaction of the NCO group in ortho position is slower. 3) An autocatalytic effect that increases the overall reaction order up to 3 is described in literature [36, 39, 41]. However, the effect is reported to be negligible in comparison to a catalyst's influence [41]; a low autocatalytic effect is reported for linear PU employing high-*M_w* polyols and HDI, leading to relatively immobile chains and low urethane concentration [40]. As the autocatalytic effect is explained with a hydrogen bond between urethane and NCO groups, it is impeded by low chain mobility (see also [42]) and, thus, not observed in this study. 4) The non-catalyzed formation of polyurethanes was excluded from the model as no additional reaction can be observed in the conversion curves and the inclusion of an additional reaction equation in the model has no effect on the fit. It is concluded that in the present case, the non-catalyzed reaction is too slow to have a noticeable influence on the overall kinetics. 5) For the experiments with stoichiometry variation, fits with Eq. (5) do not yield meaningful values of separate reaction orders and no improvement in fit quality can be observed in comparison to a simple fit with an overall reaction order. Thus, the simple model description is robust to stoichiometric changes. Though unexpected at first, one interpretation can be that the reaction rate is approximately proportional to the isocyanate concentration and largely unaffected by the polyol concentration. This behavior is observed up to a moderate excess of isocyanate (NCO/OH 2:1). A further increase in isocyanate excess could not be examined as it would entail a substantial alteration of the reaction mixture's properties, e.g., viscosity and polarity, and consequently distort the reaction system. 6) The obtained catalyst order of 0.582 when employing DBTL as catalyst is in accordance with literature [43]. Reaction heat, order, and activation energy remain unaffected; thus, this set of experiments supports the initial findings as listed in Sect. 3.2. 7) Side reactions involving either functional group that compete with the urethane formation and, thus, impede (linear) chain elongation have to be accounted for. For the

OH group, no relevant side reactions in this reaction medium can be imagined. The NCO group can particularly react in the following ways (see also [44]):

- Formation of urea from isocyanate and water is avoided with sample preparation.
- Allophanate is formed by the reaction of isocyanates with urethanes with sufficient acidity of urethane nitrogen at elevated temperatures (> 100 °C) [45].
- Trimerization of isocyanates producing isocyanurates by trend occurs at high concentrations and temperatures in absence of suitable urethanization catalysts or with alkaline catalysts [45], e.g., tertiary amines.
- Radical cross-linking between a polyol double bond and an isocyanate group are promoted by radical forming conditions, e.g., oxygen being activated by light.
- Carbamate amidation, i.e., reaction of isocyanates with urethanes, carboxylate esters, or terminal carboxylic acids, is unlikely due to low nucleophilicity and unfavorable steric configuration but cannot be excluded.

None of the presented side reactions could be observed with IR analytics. This implies that the side reactions do not occur in quantities that directly affect the main reaction's stoichiometry (similarly see [40]). As a consequence, deviations have to be attributed to other effects. Fig. 5 summarizes possible side reactions that can directly or indirectly affect the reaction rate.

4.3 Physical Effects: Mass Transport/Mobility

Mass transport can affect the kinetic behavior; two ways of which can be distinguished in this study: first, the chain length as a result of the main reaction and second, cross-linking as a result of side reactions. Ideal mixing is assumed at the beginning of the reaction. An overall reaction order of about 1 is obtained for all examined systems as opposed to an order of 2 which is reported for urethane systems applying DBTL as a homogenous catalyst [15, 36, 41]. This suggests a strong influence of the polymer chain's mobility on the reaction rate: 1) long(er) chains are relatively immobile; short(er) chains "look for" long(er) chains. 2) In addition, long(er) chains are increasingly intertwined. A general slowdown of polyurethane formation due to physical effects is reported by several authors [15, 41–43], more specifically, a deviation from second order kinetics at higher conversion or with an onset of diffusion influence (described as transition from liquid to solid) [36, 46, 47], with an example of about 1 (and low autocatalytic effect) reported by Lucio et al. [42] for a reaction of long-chain hydroxyl-terminated polybutadiene with isophorone diisocyanate. The effect is observed from the beginning of the reaction and no increase of mass transport limitations occurred over the course of the reaction. This is counter-intuitive. It is suspected that the vigorous mixing leads to substantial intertwining of the polyols and, thus, the reaction already starts in a state of very low chain mobility. For lengthy molecules, in the case

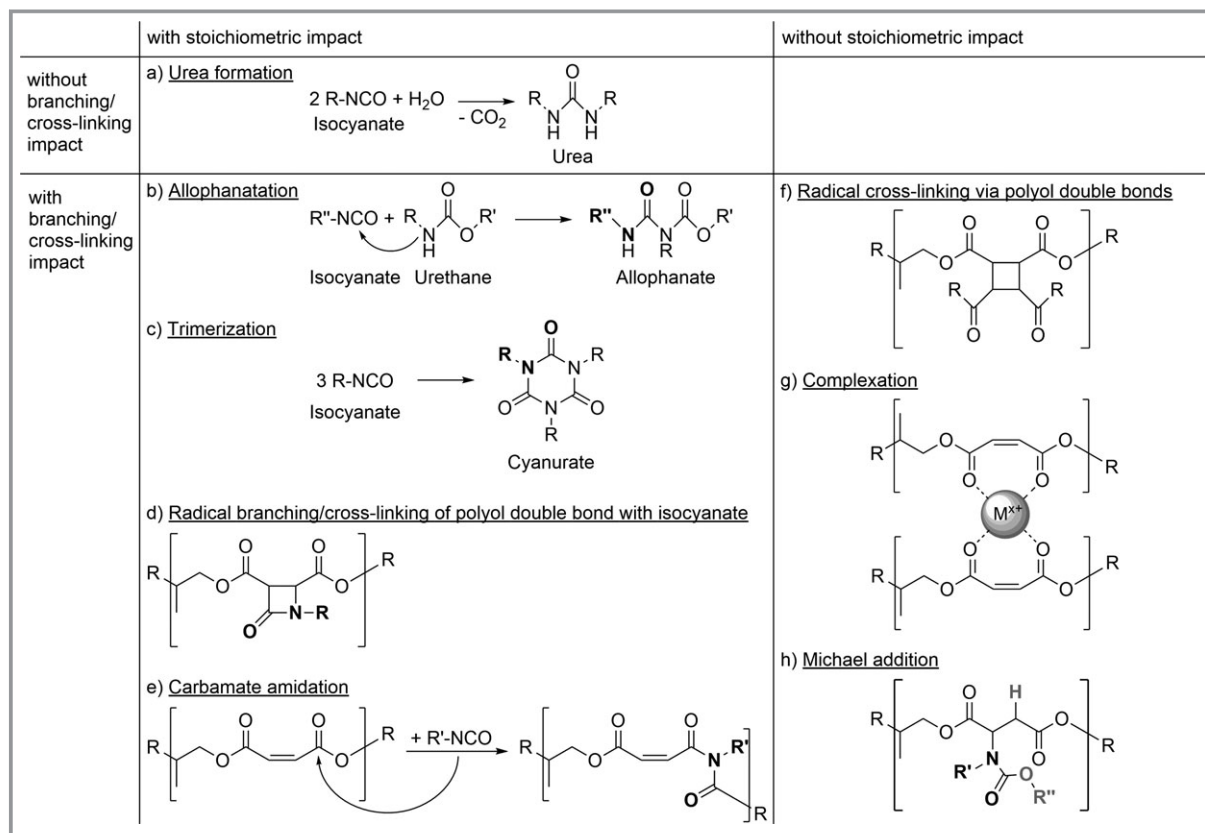


Figure 5. Possible side reactions, differentiated: with/without stoichiometric impact, with/without branching/cross-linking impact.

of thermoplastic polyurethanes (TPUs), and fast urethane reactions, especially at higher temperatures, the general assumption of functional group reactivity being independent of molecule size was reported to be questionable [43]; the experimental results shown above suggest a diffusion influence for the whole of the performed reaction.

Furthermore, there are possible side reactions that lead to branching and eventually cross-linking of the polyurethane chains. This cross-linking entails a substantial increase in viscosity and consequently a decreased mobility of the formed polymers is assumed (Stokes-Einstein equation), particularly toward high conversion. In addition to side reactions b) to e), other side reactions leading to cross-linking are possible:

- f) Radical cross-linking of two polyol double bonds is promoted by radical forming conditions, see above.
- g) Complexation of polyols with catalyst molecules forming (chelate) coordination complexes is dependent on the size, shape, and electronic properties of the catalyst.
- h) Michael addition of an isocyanate to a polyol double bond with participation of another alcohol group.

None of the reactions can be observed with IR spectrometry; they may occur in very low amounts only. A decrease in reaction rate with advanced reaction is not witnessed. Judging from the kinetic behavior of the system, no extensive

cross-linking is apparent. This holds especially true as the radical cross-linking (f), which was deemed to be the most probable direct cross-linking mechanism, is excluded after comparison with the polyol without DB (CO₂-SA-PEC) which shows nearly identical kinetic behavior.

The observed insolubility of the reacted PU samples can be a consequence of either extensive intertwining (physical reason) or cross-linking (chemical reason) or a combination of both. The polymer composition and potential cross-linking need to be examined in future research applying other analytical methods.

5 Conclusion and Outlook

In this study, the kinetics of the formation of a novel polyurethane rubber from CO₂-containing polyols was investigated. Formation kinetics of other urethanes such as foams or TPUs are well researched; however, for the newly introduced high-*M_w* polyols, which include both CO₂ and double bonds and are used in the formation of long unsaturated linear chains, i.e., rubbers, new analyses become necessary. In addition, in literature, the kinetics of polyurethanes is often examined in solution, for shorter polyols, mono-alcohols, and/or mono-isocyanates. As opposed to such

workarounds, this paper directly examined the actual industrially relevant reaction system. It was confirmed that DSC is a quick and easy way to yield a kinetic description of this complex polymer reaction.

No difference between reaction systems with and without double bonds could be observed for the kinetic parameters. Activation energies of about 53 kJ mol^{-1} with HDI, 85 kJ mol^{-1} for the ortho-positioned NCO group of TDI and 68 kJ mol^{-1} for the para-positioned NCO group of TDI were found – the latter is by trend the fastest reaction, being about 7 times as fast as the ortho-positioned NCO group and twice as fast as the HDI's NCO groups ($r_{0,\text{norm},100^\circ\text{C}}$). An overall reaction order of 2 is generally assumed for a lot of polyurethane systems. In this study, an order of about 1 was found. This suggests strong influence of the chains' low mobility, which can be seen as an onset of diffusion limitation and is due to long polymer chains and their slow diffusion in bulk.

Side reactions, especially allophanate formation and trimerization, are possible; however, none with strong direct influence on stoichiometry can be seen from the kinetic behavior and none can be observed with IR. Cross-linking between polymer chains, especially through radical cross-linking, could not be observed; minor amounts of branching or cross-linking reactions are possible but are ultimately inconsequential for the kinetic behavior of the examined systems.

It is assumed that the exact polymer composition can be affected by an actual reactor design, e.g., by shearing, and mode of operation. At the same time, it appears that for a first sizing, the kinetic behavior can be decoupled from the exact polymer composition: the obtained description allows for the selection of reaction conditions and respective residence time and, thus, enables a preliminary process design. A reactor setup could, e.g., be an extruder or plug flow tubular reactor (potentially with static mixers), or a suitable combination of both. One-shot processes including mixing in a continuously stirred tank reactor or mixing head with static mixers followed by curing (e.g., conveyer system) can also be imagined.

In future research, the analyses should be extended to different systems, i.e., polyols, diisocyanates, and catalysts, and analyzed with a wider range of methods, in particular to yield a comprehensive characterization of resulting rubbers, e.g., rheological behavior. Relevant systems depend heavily on the goal of the practitioner and will have to be discussed in strong interplay with economic considerations such as the optimization of reaction speed as a task of process design or recipe alterations to yield attractive rubber properties.

The authors would like to thank Peter Hugo (TU Berlin) for valuable leads on the analytical concept and the sample preparation, Michael Traving (Covestro) for the production of the polyols, Annika Marxen and Hanna Schachel (TU Berlin) for studies in the preparation of this work, and Michael Friedrich, Aurel Wolf, and Anna-Marie Zorn (Covestro) for fruitful discussions. The results published here have been achieved in the course of the project r+impuls "Production Dreams", FKZ 033R350A-D. The project partners gratefully acknowledge funding for this project by the German Federal Ministry of Education and Research.

Symbols used

c	[ppm]	concentration
E	[kJ mol^{-1}]	energy
F	[-]	functionality
H	[kJ mol^{-1}]	enthalpy
k	[$(\text{conc.})^{1-n}\text{s}^{-1}$]	reaction rate constant
m	[-]	reaction order (for catalyst)
M_w	[g mol^{-1}]	molecular mass
n	[-]	reaction order (for reactants)
r	[$(\text{conc.})\text{s}^{-1}$]	reaction rate
R	[$\text{J mol}^{-1}\text{K}^{-1}$]	gas constant
t	[s]	time
T	[K]	temperature
X	[-]	conversion
Z	[$(\text{conc.})^{1-n}\text{s}^{-1}$]	pre-exponential factor

Greek letters

ε	[$\text{m}^2\text{mol}^{-1}$]	molar attenuation coefficient
λ	[-]	stoichiometric factor
ν	[-]	stretching vibration
τ	[-]	transmittance

Sub- and Superscripts

'	indicator for adjusted pre-exponential factor
0	initial
A	activation
as	asymmetric
cat	catalyst
norm	normalized
R	reaction
s	symmetric

Abbreviations

DB	double bond
DBTL	dibutyltin dilaureate
DMC	double metal cyanide
DSC	differential scanning calorimetry
FTIR	Fourier transform infrared
HDI	hexamethylene diisocyanate
MA	maleic anhydride
MDI	methylene diphenyl diisocyanate
mPG	monomeric propylene glycol
PEC	polyether carbonate polyol
PO	propylene oxide
PU	polyurethane
SA	succinic anhydride
TDI	toluene diisocyanate
TPU	thermoplastic polyurethane

References

- [1] *Carbon Dioxide Utilisation – Closing the Carbon Cycle* (Eds: P. Styring, E. A. Quadrelli, K. Armstrong), 1st ed., Elsevier, Amsterdam **2014**.
- [2] J. Artz, T. E. Müller, K. Thenert, J. Kleinekorte, R. Meys, A. Sternberg, A. Bardow, W. Leitner, *Chem. Rev.* **2018**, *118* (2), 434–504. DOI: <https://doi.org/10.1021/acs.chemrev.7b00435>
- [3] *Global Roadmap for Implementing CO₂ Utilization*, Global CO₂ Initiative, Ann Arbor, MI **2016**.
- [4] J. Langanke, A. Wolf, J. Hofmann, K. Böhm, M. A. Subhani, T. E. Müller, W. Leitner, C. Gürtler, *Green Chem.* **2014**, *16* (4), 1865–1870. DOI: <https://doi.org/10.1039/c3gc41788c>
- [5] T. E. Müller, C. Gürtler, A. M. Subhani, Method for Manufacturing Polyether Carbonate Polyols, *EP2604642A1*, **2011**.
- [6] C. Gürtler, *Int. Conf. on Carbon Dioxide Utilization*, Plenary Lecture LT1, Sheffield, September **2016**.
- [7] J. Norwig, *Macromolecular Colloquium Freiburg*, Freiburg, February **2017**.
- [8] J. Norwig, *11th Int. Conf. on Bio-based Materials*, Cologne, May **2018**.
- [9] C. Hopmann, A. Lipski, *KGK* **2017**, *9*, 28–31.
- [10] D. Threadingham, W. Obrecht, W. Wieder, G. Wachholz, R. Engenhausen, *Rubber*, 3. *Synthetic Rubbers, Introduction and Overview*, in Ullmann's Encyclopedia of Industrial Chemistry, Wiley-VCH, Weinheim **2011**. DOI: https://doi.org/10.1002/14356007.a23_239.pub5
- [11] A. Scott, *Chem. Eng. News* **2015**, *93* (45), 10–16. <https://cen.acs.org/articles/93/i45/Learning-Love-CO2.html>
- [12] S. Braun, H. Zwick, M. Wohak, J. Hofmann, A. Wolf, M. Traving, R. Bachmann, Method for Producing Polyether Carbonate Polyols and Device for the Same, *EP3164441B1*, **2015**.
- [13] J. Hofmann, S. Braun, A. Wolf, Method for Manufacturing Polyether Carbonate Polyols, *EP3219741A1*, **2016**.
- [14] J. Norwig, *CroCO₂PETs: Cross-linkable CO₂-Polyether Polyols*, Climate-KIC Germany, Berlin **2016**. <http://enco2re.climate-kic.org/projects/croco2pets/>
- [15] W. Sultan, J. P. Busnel, *J. Therm. Anal. Calorim.* **2006**, *83* (2), 355–359. DOI: <https://doi.org/10.1007/s10973-005-7026-8>
- [16] S. Vyazovkin, *Int. J. Chem. Kinet.* **1996**, *28* (2), 95–101. DOI: [https://doi.org/10.1002/\(SICI\)1097-4601\(1996\)28:2<95::AID-KIN4>3.0.CO;2-G](https://doi.org/10.1002/(SICI)1097-4601(1996)28:2<95::AID-KIN4>3.0.CO;2-G)
- [17] P. Hugo, *Chem. Ing. Tech.* **1993**, *65* (12), 1497–1500. DOI: <https://doi.org/10.1002/cite.330651215>
- [18] M. F. Sonnenschein, *Polyurethanes: Science, Technology, Markets, and Trends*, John Wiley & Sons, Hoboken, NJ **2015**.
- [19] J. Leonhardt, P. Hugo, *J. Therm. Anal.* **2005**, *49* (3), 1535–1551. DOI: <https://doi.org/10.1007/bf01983714>
- [20] G. W. H. Höhne, W. F. Hemminger, H.-J. Flammersheim, *Differential Scanning Calorimetry*, 2nd ed., Springer, Heidelberg **2003**.
- [21] L. I. Kopusov, V. V. Zharkov, *J. Appl. Spectrosc.* **1966**, *5* (1), 95–97. DOI: <https://doi.org/10.1007/bf00604661>
- [22] K. Nakayama, T. Ino, I. Matsubara, *J. Macromol. Sci., Part A: Chem.* **1969**, *3* (5), 1005–1020. DOI: <https://doi.org/10.1080/10601326908051929>
- [23] R. W. Seymour, G. M. Estes, S. L. Cooper, *Macromolecules* **1970**, *3* (5), 579–583. DOI: <https://doi.org/10.1021/ma60017a021>
- [24] F. Papadimitrakopoulos, W. J. MacKnight, E. Sawa, *Macromolecules* **1992**, *25* (18), 4682–4691. DOI: <https://doi.org/10.1021/ma00044a033>
- [25] M. Sato, T. Xi, A. Nakamura, Y. Kawasaki, T. Umemura, M. Tsuda, Y. Kurokawa, *J. Biomed. Mater. Res.* **1995**, *29* (10), 1201–1213. DOI: <https://doi.org/10.1002/jbm.820291007>
- [26] L. S. Teo, C. Y. Chen, J. F. Kuo, *Macromolecules* **1997**, *30* (6), 1793–1799. DOI: <https://doi.org/10.1021/ma961035f>
- [27] J. A. Hiltz, *Characterization of Poly(ether)urethane Thermoplastic Elastomers*, Technical Memorandum 98/222, Defence Research Establishment Atlantic, Dartmouth, NS **1998**.
- [28] A. Asefnajad, M. Taghi Khorasani, A. Behnamghader, B. Farsadzadeh, S. Bonakdar, *Int. J. Nanomed.* **2011**, *6*, 2375–2384. DOI: <https://doi.org/10.2147/IJN.S15586>
- [29] M. Rogulska, A. Kultys, E. Olszewska, *J. Therm. Anal. Calorim.* **2013**, *114* (2), 903–916. DOI: <https://doi.org/10.1007/s10973-013-3007-5>
- [30] E. S. Jamadi, L. Ghasemi-Mobarakeh, M. Morshed, M. Sadeghi, M. P. Prabhakaran, S. Ramakrishna, *Mater. Sci. Eng., C* **2016**, *63*, 106–116. DOI: <https://doi.org/10.1016/j.msec.2016.02.051>
- [31] M. A. Garrido, R. Font, *J. Anal. Appl. Pyrolysis* **2015**, *113*, 202–215. DOI: <https://doi.org/10.1016/j.jaap.2014.12.017>
- [32] L. Kong, F. Qiu, Z. Zhao, X. Zhang, T. Zhang, J. Pan, D. Yang, *J. Cleaner Prod.* **2016**, *137*, 51–59. DOI: <https://doi.org/10.1016/j.jclepro.2016.07.067>
- [33] R. H. Li, T. A. Barbari, *J. Membr. Sci.* **1996**, *111* (1), 115–122. DOI: [https://doi.org/10.1016/0376-7388\(95\)00296-0](https://doi.org/10.1016/0376-7388(95)00296-0)
- [34] M. A. Hood, B. Wang, J. M. Sands, J. J. La Scala, F. L. Beyer, C. Y. Li, *Polymer* **2010**, *51* (10), 2191–2198. DOI: <https://doi.org/10.1016/j.polymer.2010.03.027>
- [35] R. Merten, D. Lauerer, G. Braun, M. Dahm, *Makromol. Chem.* **1967**, *101* (1), 337–366. DOI: <https://doi.org/10.1002/macp.1967.021010119>
- [36] J. L. Han, C. H. Yu, Y. H. Lin, K. H. Hsieh, *J. Appl. Polym. Sci.* **2008**, *107* (6), 3891–3902. DOI: <https://doi.org/10.1002/app.27421>
- [37] P. Yang, T. Li, J. Li, *Int. J. Chem. Kinet.* **2013**, *45* (10), 623–628. DOI: <https://doi.org/10.1002/kin.20798>
- [38] I. Yilgor, B. D. Mather, S. Unal, E. Yilgor, T. E. Long, *Polymer* **2004**, *45* (17), 5829–5836. DOI: <https://doi.org/10.1016/j.polymer.2004.05.026>
- [39] P. Król, *Prog. Mater. Sci.* **2007**, *52* (6), 915–1015. DOI: <https://doi.org/10.1016/j.pmatsci.2006.11.001>
- [40] B. Fernandez d'Arlas, L. Rueda, P. M. Stefani, K. de la Caba, I. Mondragon, A. Eceiza, *Thermochim. Acta* **2007**, *459* (1–2), 94–103. DOI: <https://doi.org/10.1016/j.tca.2007.03.021>
- [41] J. M. E. Rodrigues, M. R. Pereira, A. G. De Souza, M. L. Carvalho, A. A. Dantas Neto, T. N. C. Dantas, J. L. C. Fonseca, *Thermochim.*

- Acta* **2005**, *427* (1–2), 31–36. DOI: <https://doi.org/10.1016/j.tca.2004.08.010>
- [42] B. Lucio, J. L. De La Fuente, *Thermochim. Acta* **2016**, *625*, 28–35. DOI: <https://doi.org/10.1016/j.tca.2015.12.012>
- [43] V. W. A. Verhoeven, A. D. Padsalgikar, K. J. Ganzeveld, L. P. B. M. Janssen, *J. Appl. Polym. Sci.* **2006**, *101* (1), 370–382. DOI: <https://doi.org/10.1002/app.23848>
- [44] R. G. Arnold, J. A. Nelson, J. J. Verbanc, *Chem. Rev.* **1957**, *57* (1), 47–76. DOI: <https://doi.org/10.1021/cr50013a002>
- [45] N. Ketata, C. Sanglar, H. Waton, S. Alamercery, F. Delolme, O. Paise, G. Raffin, M. F. Grenier-Loustalot, *Polym. Polym. Compos.* **2004**, *12* (8), 645–665. DOI: <https://doi.org/10.1177/096739110401200801>
- [46] S. Li, R. Vatanparast, H. Lemmetyinen, *Polymer* **2000**, *41* (15), 5571–5576. DOI: [https://doi.org/10.1016/S0032-3861\(99\)00785-5](https://doi.org/10.1016/S0032-3861(99)00785-5)
- [47] S. Parnell, K. Min, M. Cakmak, *Polymer* **2003**, *44* (18), 5137–5144. DOI: [https://doi.org/10.1016/S0032-3861\(03\)00468-3](https://doi.org/10.1016/S0032-3861(03)00468-3)